Liquid–Liquid Phase Separation and Crystallization of Polydisperse Isotactic Polypropylene Solutions

HWAN KWANG LEE,[1] SUNG CHUL KIM,[2] KALLE LEVON[3]

[1] Department of Industrial Chemistry, Chungnam Sanup University, #29, Namjang-Ri, Hongsung-Eub, Hongsung-Gun, Chungnam 350-800, Korea

[2] Department of Chemical Engineering, Korea Advanced Institute of Science and Technology, 373-1, Kusong-Dong, Yusung-Gu, Taejon 305-701, Korea

[3] Department of Chemical Engineering, Chemistry, and Materials Science, Polytechnic University, Six Metrotech Center, Brooklyn, New York 11201, USA

Received September 1997; accepted 16 November 1997

ABSTRACT: Phase diagrams were calculated based on Flory-Huggins solution thermodynamics to investigate the effects of polydispersity of polymer molecules and interaction parameter on the phase equilibria of crystallizable polymer solutions. The polydispersity was modeled with blends of two monodisperse polymers differing in chain lengths as a simplification. It was found that a longer chain length component could be separated easily to a polymer-rich phase by liquid demixing, but a shorter chain length component might exist at relatively constant concentration in each phase on fractionation. The influence of polydispersity on the liquid–solid phase equilibrium was small, and the phase boundary could be moved significantly in the region of low concentration of polymer by a small change of temperature. Liquid–liquid phase separation was more sensitive to the interaction between polymer and solvent than liquid–solid phase transition. Numerical calculations showed that the temperature at which liquid–liquid phase separation was coupled with liquid–solid phase equilibrium increased with a lower concentration of the polymer due to polydispersity of polymer chain lengths, and this phenomenon was observed at a lower temperature with more favorable interaction. The results were consistent with the experimental observations of isotactic polypropylene solutions. © 1998 John Wiley & Sons, Inc. J Appl Polym Sci 70: 849–857, 1998

Key words: Liquid–liquid phase separation; crystallization; polydispersity; interaction parameter; isotactic polypropylene solution

INTRODUCTION

Thermally induced phase separation (TIPS) is one of the major processes to produce microporous polymeric membranes.[1–4] In the TIPS process a homogeneous polymer solution may undergo phase separation into a polymer-rich phase and a polymer-lean phase by lowering the temperature, the system of which is termed as an upper critical solution temperature (UCST) type. The solidification of the solution to fix the structure can be achieved by vitrification of the polymer-rich phase,[5] crystallization of the polymer,[6,7] and freezing of the solvent[8] at a certain stage during liquid–liquid (L-L) demixing. Consequently understanding the interplay of L-L demixing and these transitions is a key to con-

Correspondence to: H. K. Lee
Contract grant sponsor: Chungnam Sanup University.

Journal of Applied Polymer Science, Vol. 70, 849–857 (1998)
 CCC 0021-8995/98/050849-09

trol the morphology and to interpret the membrane structure.

In this study we are concerned with the interference of L-L phase separation and crystallization of the polymer in polydisperse polymer solutions. This work was motivated by the anomalous phase behavior of isotactic polypropylene (i-PP) solutions showing that melting temperatures were elevated with decreasing polymer concentration when L-L phase separation preceded crystallization on cooling.[9] The same phenomenon was reported by Aerts et al. for polyethylene–diphenyl ether systems.[10] Similar elevation of vitrification curves due to polydispersity was observed by Vandeweerdt et al. for atactic poly(methyl methacrylate) solutions.[11]

In this article, phase diagrams based on the Flory-Huggins theory were calculated to investigate the effects of the polydispersity of polymer molecules and interaction parameter on the phase equilibria of crystallizable polymer solutions. The polydispersity was modeled with blends of two monodisperse polymers differing in chain lengths as a simplification. The interference of L-L phase separation and crystallization of i-PP solutions in dialkyl phthalate was qualitatively interpreted with the computed phase diagrams.

THEORY

The influence of the polydispersity of polymer molecules on phase equilibria in this manuscript was investigated by the Flory-Huggins lattice treatment[12,13] with ternary solutions comprising blends of two monodisperse polymers differing in only chain lengths, dissolved in one solvent. This type of system was commonly used to model polydispersity in phase behavior of polymer solutions.[14–16] Because the use of two monodisperse fractions of different molecular weight is a simplification to represent a polymer sample of broad molecular weight distribution, the results obtained with this model are not expected to fit the experimental data quantitatively.[15,17] Nevertheless ternary phase diagrams are very elucidative and explicitly reveal the differences in behavior between binary and ternary systems.

Liquid–Liquid Phase Equilibrium

If it is assumed that the interaction parameter between two homologous polymers is zero and that the interactions between each polymer and the solvent are identical, the free energy of mixing ΔG_M in ternary solutions is given by

$$\frac{\Delta G_M}{RT} = n_0 \ln \phi_0 + n_1 \ln \phi_1 + n_2 \ln \phi_2 + \chi\, n_0(\phi_1 + \phi_2) \quad (1)$$

where n_i are mol of component i, ϕ_i is the volume fraction of component i, χ is the interaction parameter between the solvent and polymer, and R and T have the usual significance. The subscript 0 refers to the solvent, and subscripts 1 and 2 refer to the polymer. The molecular weight of polymer2 is considered to be greater than that of polymer1 in the above equation. The interaction parameter is assumed to be dependent only of temperature and the relation of $\chi = \alpha + \beta/T$ is used, as is often the case for polymer solutions.[12] When the proper derivatives of the free energy of mixing are taken, the chemical potential of component i, $\Delta\mu_i$ may be written as

$$\frac{\Delta\mu_0}{RT} = \ln \phi_0 + 1 - \phi_0 - \phi_1\left(\frac{\nu_0}{\nu_1}\right) - \phi_2\left(\frac{\nu_0}{\nu_2}\right) + \chi\,(\phi_1 + \phi_2)^2 \quad (2)$$

$$\frac{\Delta\mu_1}{RT} = \ln \phi_1 + 1 - \phi_1 - \phi_0\left(\frac{\nu_1}{\nu_0}\right) - \phi_2\left(\frac{\nu_1}{\nu_2}\right) + \chi\phi_0^2\left(\frac{\nu_1}{\nu_0}\right) \quad (3)$$

$$\frac{\Delta\mu_2}{RT} = \ln \phi_2 + 1 - \phi_2 - \phi_0\left(\frac{\nu_2}{\nu_0}\right) - \phi_1\left(\frac{\nu_2}{\nu_1}\right) + \chi\phi_0^2\left(\frac{\nu_2}{\nu_0}\right) \quad (4)$$

where ν_i is the molar volume of component i. The condition for equilibrium between two liquid phases I and II is

$$\Delta\mu_i^{\mathrm{I}} = \Delta\mu_i^{\mathrm{II}} \ (i = 0,\ 1,\ 2) \quad (5)$$

and the material balance requires

$$\sum \phi_i^{\mathrm{I}} = \sum \phi_i^{\mathrm{II}} = 1 \quad (6)$$

Superscripts I and II refer to polymer-rich and polymer-lean phases, respectively.

Given the χ value (or temperature), selection of one of the compositions as an independent variable leaves five coupled nonlinear equations to be solved for the individual tie lines. In our calculation ϕ_2^{II} was selected as the independent variable. The Newton-Raphson method, based on a least-squares procedure, was employed to solve the simultaneous equations.[18,19]

Liquid–Solid Phase Equilibrium

Crystalline–liquid equilibrium requires that the chemical potentials of each crystallizable component for the crystalline phase and for the solution phase are identical.

$$\Delta\mu_i^C = \Delta\mu_i^L \ (i = 1, 2) \tag{7}$$

Superscripts C and L refer to crystalline and liquid phases, respectively. Using the expressions for the free energy of fusion with a certain approximation,[12] one can obtain the following expressions for the chemical potentials of polymer1 and polymer2 in the crystalline phase

$$\Delta\mu_1^C = -\phi_1^C \Delta H_u \left(1 - \frac{T}{T_m^\circ}\right)\left(\frac{\nu_1}{\nu_0}\right) \tag{8}$$

$$\Delta\mu_2^C = -\phi_2^C \Delta H_u \left(1 - \frac{T}{T_m^\circ}\right)\left(\frac{\nu_2}{\nu_0}\right) \tag{9}$$

where ΔH_u is the heat of fusion of the polymer repeating unit, and T and T_m° are the melting temperature of the polymer in the solution and of the pure polymer, respectively. T_m° is assumed to be independent of the molar size of the polymer, and the temperature dependence of $\chi = \alpha + \beta/T$ is used. From the material balance, one has

$$\phi_1^C + \phi_2^C = 1 \tag{10}$$

The chemical potentials of polymer1 and polymer2 for the liquid phase are evaluated by eqs. (3) and (4), respectively.

Given temperature, one has four coupled equations, including two equations of material balance and five variables of composition. Selection of one of the compositions as an independent variable allows one to solve the nonlinear algebraic equations, and the tie line of solid–liquid equilibrium can be obtained. We selected ϕ_2^L as the independent variable. The Newton-Raphson method was again employed to solve the equations.

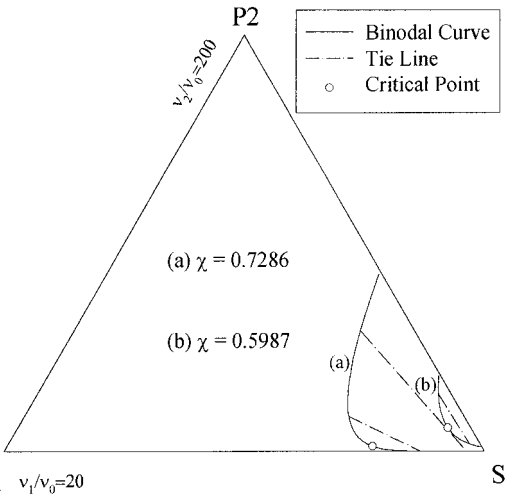

Figure 1 Binodal compositions and tie lines for χ = 0.7286 (a) and χ = 0.5987 (b) with ν_1/ν_0 = 20 and ν_2/ν_0 = 200.

CALCULATION RESULTS AND DISCUSSION

The ternary phase diagrams showing L-L phase equilibrium for hypothetical polymer solutions, comprised of two monodisperse polymers differing in chain lengths and a solvent, are illustrated in Figures 1–3. Each vertex denotes the pure component; S for solvent, P1 for polymer1, and P2 for polymer2. To investigate the effect of polydispersity, the value of ν_2/ν_0 (molar volume ratio of higher molecular weight polymer to solvent) was increased from 200 to 20,000, with a value of 20 for ν_1/ν_0 (molar volume ratio of lower molecular weight polymer to solvent) at given interaction parameter χ. The effect of temperature on L-L phase separation could be explained in terms of temperature dependence of the χ value. For a typical i-PP system[20] exhibiting $\chi = -0.7 + 500/T$, the corresponding temperature in Figures 1–3 is 350 K with χ = 0.7286 and 385 K with χ = 0.5987.

It is seen in Figures 1–3 that the L-L phase separation gap is decreased with a smaller χ value for given values of ν_1/ν_0 and ν_2/ν_0. The region of two phases is enlarged with greater value of ν_2/ν_0 for constant χ, and this is more pronounced with a strong solvent power, i.e., for a

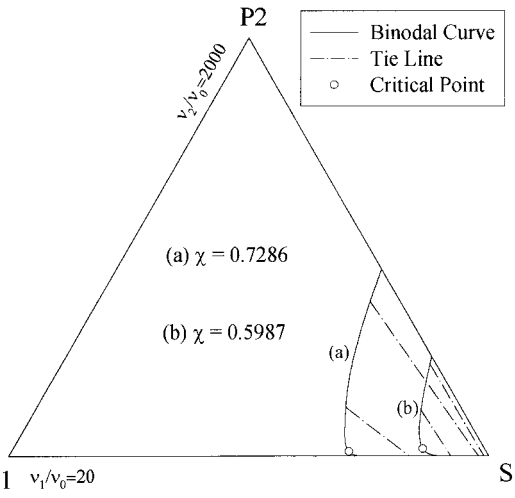

Figure 2 Binodal compositions and tie lines for χ = 0.7286 (a) and χ = 0.5987 (b) with ν_1/ν_0 = 20 and ν_2/ν_0 = 2000.

smaller χ value. The effect of ν_2/ν_0 on the binodal curve becomes apparently small when the value of ν_2/ν_0 is large, as can be observed in Figures 2 and 3. The critical composition in ternary phase diagrams becomes located closer to the axis of lower molecular weight polymer–solvent with larger ν_2/ν_0, which indicates that the component of longer chain length can be separated easily to the polymer-rich phase by liquid demixing for a mixture of dissimilar chain lengths. However, the shorter chain length component would exist at relatively constant concentration in each phase on fractionation because the tie line is almost parallel to the axis of higher molecular weight polymer–solvent.

The cloud–point curve of a pseudobinary solution may be constructed from ternary phase diagrams. The line between the vertex S and a point at P1–P2 axis in Figure 1 represents a constant ratio of the two polymers at varying total polymer concentrations. The intersections of this line and binodal curves with varying χ values (varying temperatures) constitute the phase diagram of the pseudobinary solution. In general the highest precipitation temperature is not the critical point, as it is in a truly binary system.[15,21]

The composition curves for liquid–solid equilibrium as a function of temperature are shown in Figures 4 and 5, in which the relevant parameters were taken from typical values for i-PP systems.[20,22] The overall feature is that the phase transition curve is parallel to P1–P2 axis in the region of high concentration of the polymer, and the location of the phase boundary changes significantly with a small drop of temperature in less concentrated solution. In a pseudobinary solution of 50/50 P1/P2, which is represented by the line connecting the center of P1–P2 axis and the vertex S, for instance, the melting point is 333 K for 50 vol % of total polymer concentration and 315 K for 10 vol % of total polymer concentration, with $\chi = -0.7 + 400/T$ in Figure 4(a). Thus, the dilution to 50% gives rise to a melting point depression of 114 K and the dilution to 10% does of 132 K (the melting temperature of the pure polymer is 447 K).

Comparison between Figures 4 and 5 reveals that the melting point of the polymer blend is influenced by interaction parameter. When temperature dependence of interaction parameter is $\chi = -0.7 + 500/T$ in Figure 5(a), the melting point is 347 K for 50 vol % of total polymer concentration and 342 K for 10 vol % of total polymer concentration in the pseudobinary solution of a 50/50 P1/P2 blend, which indicates that the unfavorable interaction gives rise to a less amount of melting point depression at a given concentration of total polymer. The location of the phase transition curve changes negligibly when the value of ν_2/ν_0 is increased from 200 to 20,000, as can be observed in Figures 4 and 5. This suggests the effect of the polydispersity of polymer chain lengths on liquid–solid phase equilibrium is small, which is in accord with the experimental observations of linear polyethylene systems.[23,24]

It should be noted that interaction parameter influences L-L phase separation temperature

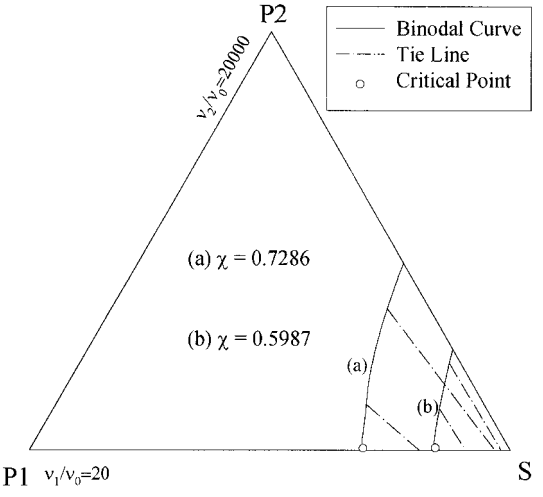

Figure 3 Binodal compositions and tie lines for χ = 0.7286 (a) and χ = 0.5987 (b) with ν_1/ν_0 = 20 and ν_2/ν_0 = 20,000.

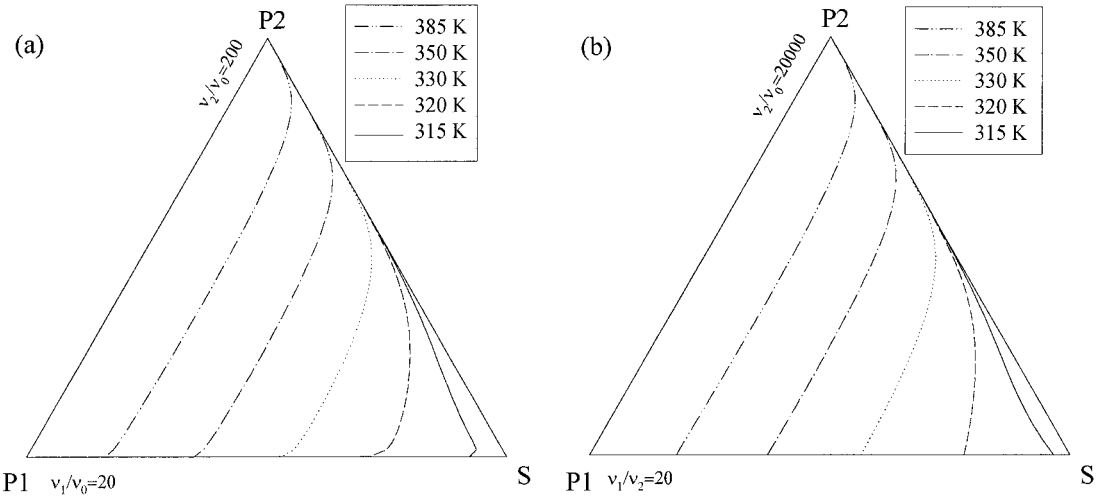

Figure 4 Crystalline–liquid phase equilibrium composition curves as a function of temperature for ΔH_u = 8790 J/mol, T_m° = 447 K, and $\chi = -0.7 + 400/T$ with ν_1/ν_0 = 20 and ν_2/ν_0 = 200 (a), and with ν_1/ν_0 = 20 and ν_2/ν_0 = 20,000 (b).

more significantly than liquid–solid phase transition temperature, as summarized in Table I. The binodal concentration of the 50/50 P1/P2 blend with ν_1/ν_0 = 20 and ν_2/ν_0 = 200 in Figure 1 is 38 vol % for χ = 0.7286, which is higher than the critical concentration of the polymer solution (ϕ_{cr}), and the corresponding higher value of the polymer solution is 9 vol % for χ = 0.5987, which is less than ϕ_{cr}. The difference in L-L phase separation temperature due to change in temperature dependence of the interaction parameter from $\chi = -0.7 + 400/T$ to $\chi = -0.7 + 500/T$ is in the range of 70–77 K for the range of χ values considered in Figure 1. The corresponding values for the liquid–solid equilibrium are 14 K for 50% solution and 27 K for 10% solution, as indicated in Table I. Similar trends in binary system were reported by Burghardt.[25]

In simultaneous phase transitions L-L phase separation and liquid–solid phase transition may take place competitively. Such a situation can be readily achieved where the concentration of the total polymer is less than ca. 50% by properly selected temperature dependence of χ for given

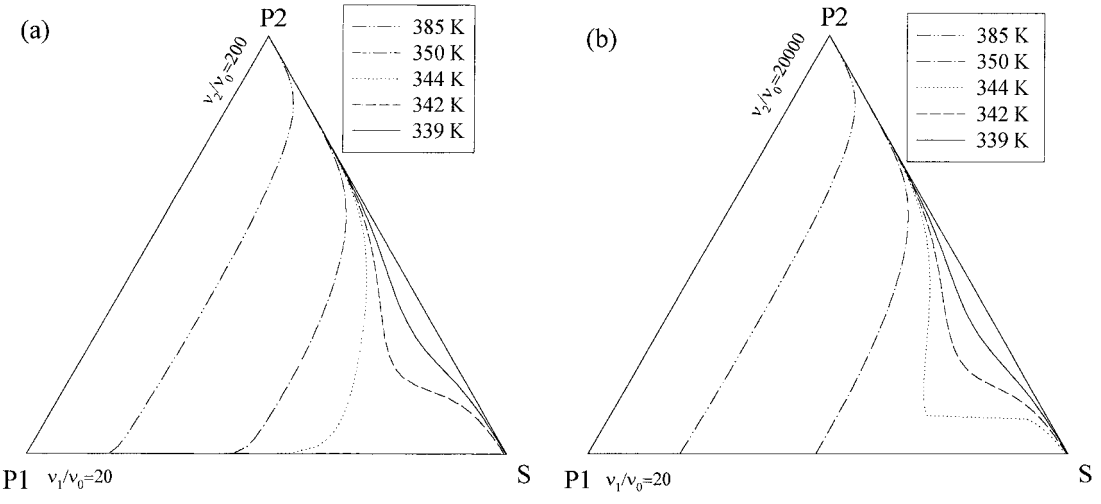

Figure 5 Crystalline–liquid phase equilibrium composition curves as a function of temperature for ΔH_u = 8790 J/mol, T_m° = 447 K, and $\chi = -0.7 + 500/T$ with ν_1/ν_0 = 20 and ν_2/ν_0 = 200 (a), and with ν_1/ν_0 = 20 and ν_2/ν_0 = 20,000 (b).

Table I Effects of Interaction Parameter on L-L Phase Equilibrium and Liquid–Solid (L-S) Phase Equilibrium Temperatures for Pseudobinary Solution of 50/50 P1/P2 Blend with ΔH_u = 8790 J/mol, T_m° = 447 K, ν_1/ν_0 = 20 and ν_2/ν_0 = 200

	Volume % of Polymer Blend	T_1 (K) in $\chi = -0.7 + 400/T_1$	T_2 (K) in $\chi = -0.7 + 500/T_2$	$T_2 - T_1$ (K)
L-L	38 ($\phi_1 + \phi_2 > \phi_{cr}$)	280	350	70
	9 ($\phi_1 + \phi_2 < \phi_{cr}$)	308	385	77
L-S	50	333	347	14
	10	315	342	27

crystallizable polymer blends where the liquid–solid phase boundary can be extensively moved with a change of a few degrees of temperature, as shown in Figures 4 and 5. This may be experimentally realized by controlling the interaction between the polymer and solvent through proper selection of the solvent in binary polymer–solvent mixtures,[9] or by controlling the composition of solvent mixtures in ternary polymer solutions,[7] because the L-L phase boundary is more sensitive to solvent power than the liquid–solid phase boundary.

Phase diagrams as a function of temperature in which binodal curves were superimposed upon liquid–solid phase transition curves with $\chi = -0.7 + 480/T$ for $\nu_1/\nu_0 = 20$ and $\nu_2/\nu_0 = 200$ are shown in Figure 6. At 341 K the two types of phase transition curves do not cross, but do intersect each other below 339 K. As the temperature decreases, the solvent concentration where two types of phase transitions coincide decreases in Figure 6. This can be interpreted that the temperature at which liquid–solid phase transition coupled with liquid demixing increases with a decrease of total polymer concentration. The liquid–solid phase transition curve inside the L-L phase separation gap is not valid and should be replaced by the tie line located at the intersection of the two types of phase transitions.

With more favorable interaction between polymer and solvent, the onset temperature to obtain the coupled phase separation shifts to a lower value, as shown in Figure 7. The simultaneous phase separation starts to occur at 339 K, with $\chi = -0.7 + 480/T$ in Figure 6, and at 335 K with $\chi = -0.7 + 470/T$ in Figure 7. When the value

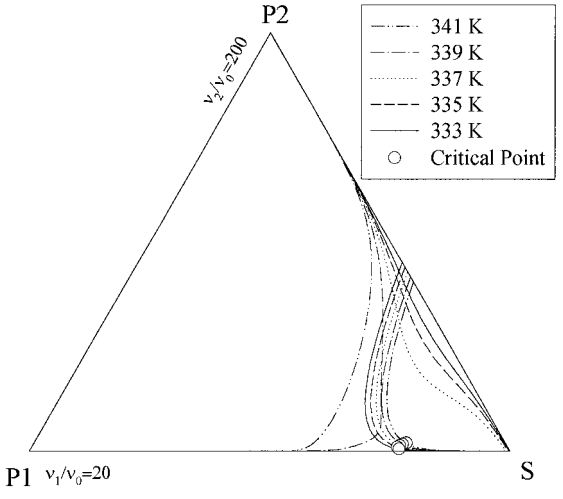

Figure 6 Binodal compositions and crystalline–liquid phase equilibrium compositions as a function of temperature for ΔH_u = 8790 J/mol, T_m° = 447 K, and $\chi = -0.7 + 480/T$ with ν_1/ν_0 = 20 and ν_2/ν_0 = 200.

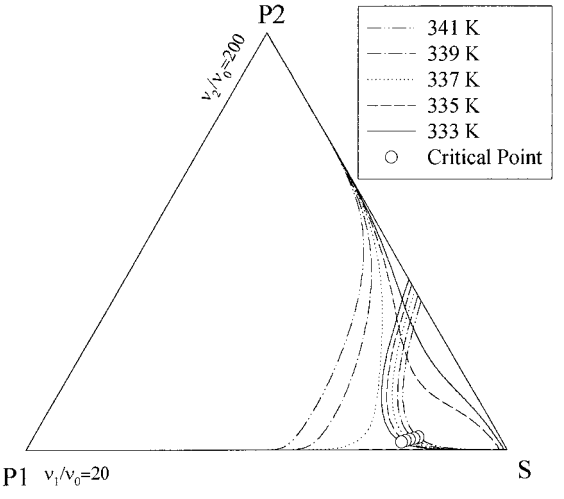

Figure 7 Binodal compositions and crystalline–liquid phase equilibrium compositions as a function of temperature for ΔH_u = 8790 J/mol, T_m° = 447 K, and $\chi = -0.7 + 470/T$ with ν_1/ν_0 = 20 and ν_2/ν_0 = 200.

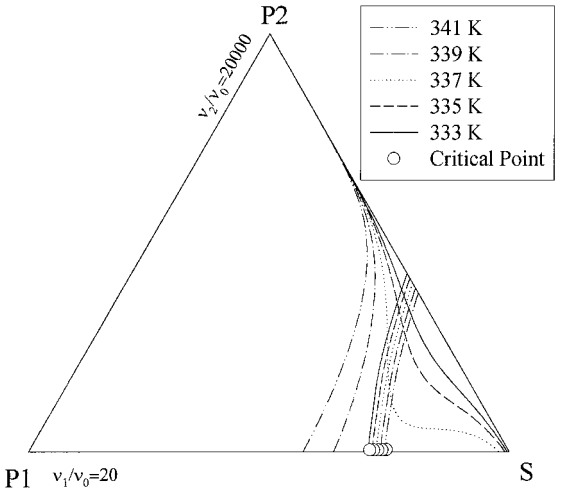

Figure 8 Binodal compositions and crystalline–liquid phase equilibrium compositions as a function of temperature for $\Delta H_u = 8790$ J/mol, $T^{\circ}_m = 447$ K, and $\chi = -0.7 + 470/T$ with $\nu_1/\nu_0 = 20$ and $\nu_2/\nu_0 = 20{,}000$.

of ν_2/ν_0 is increased to 20,000 at the same interaction parameter, the simultaneous phase transition starts to occur on cooling at 337 K in Figure 8, which is a slightly higher temperature than for the case of $\nu_2/\nu_0 = 200$. This phenomenon is opposite to the effect of the favorable interaction. A higher molecular weight of polymer2 enlarges liquid demixing gap and shifts liquid–solid phase transition to the region of lower concentration of polymer blends.

EXPERIMENTAL

A commercial grade of i-PP (Exxon PD020) with M_w of 4.4×10^5 and M_w/M_n of 6.8 was used. A series of 1,2-dialkyl phthalates, designated as C4 (dibutyl), C6 (dihexyl), C7 (diheptyl), and C8b (di-2-ethylhexyl) was used to control the interaction between polymer and solvent. Observation of L-L phase separation temperature ($T_{\text{L-L}}$) was followed by optical microscopy (Nikon HFX II) with a hot stage (Mettler FP82) at a cooling rate of 10°C/min. Peak-melting temperature (T_m) and onset-crystallization temperature (T_{cry}) were determined by differential scanning calorimetry (Perkin-Elmer DSC-7) at a scanning rate of 10°C/min. The experimental details were described elsewhere.[9]

Melting temperature curves for i-PP solutions in a series of phthalates are shown in Figure 9. In a good solvent of C8b phthalate the melting temperature decreased monotonically with dilution, as is the usual case, but in worse solvents containing a shorter alkyl chain in phthalate the melting temperature started to increase at a certain concentration of i-PP. Figure 10 indicates that the region where melting point deviates from expectation corresponds to the region where L-L phase separation precedes crystallization on cooling. Optical microscopy confirmed that in the C8b system L-L phase separation was not observed before crystallization. It is understood that the anomalous melting behavior may be related to the effect of polydispersity of polymer molecules on the coupled phase transition. Thus, during a DSC run a high molecular weight fraction is precipitated from the mother solution and, subsequently, the polymer-rich phase is crystallized. The deviation of the melting point was not observed for the i-PP samples of narrow molecular weight distribution when the L-L phase separation preceded crystallization on cooling.[9] The elevation of crystallization temperature with dilution is not clearly observed for i-PP solutions in C6 and C7 phthalates in Figure 10. In these cases the L-L phase separation might not give rise to a sufficient fractionation prior to the onset of crystallization because liquid demixing and crystallization occurred in narrow temperature ranges.

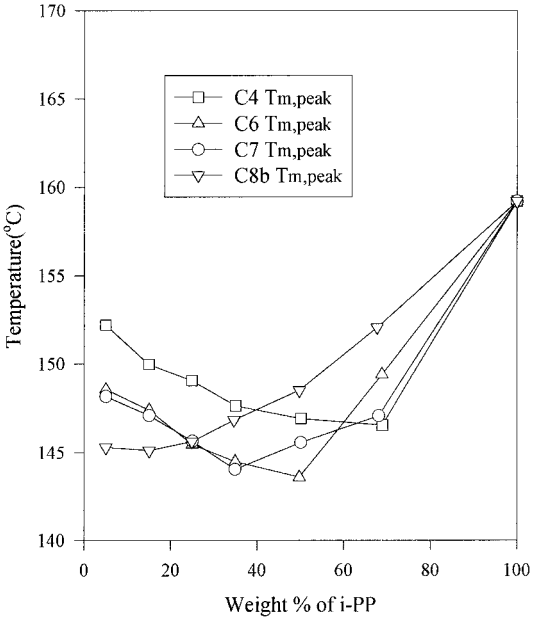

Figure 9 Peak-melting temperature curves measured by DSC at a heating rate of 10°C/min for solutions of i-PP and phthalates of dibutyl (C4), dihexyl (C6), diheptyl (C7), and di-2-ethylhexyl (C8b).

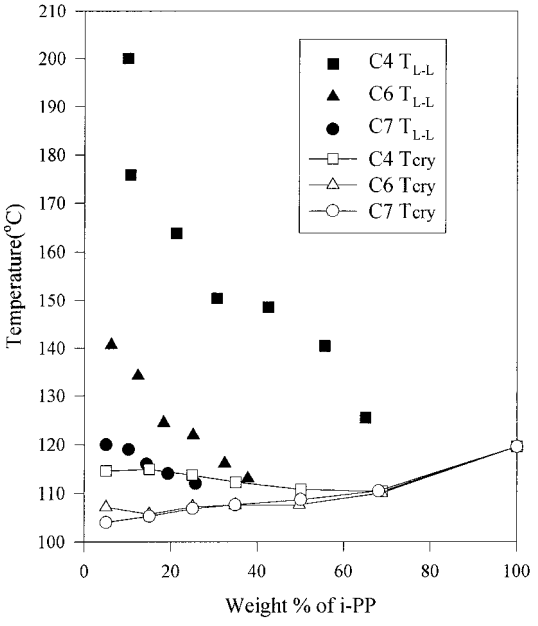

Figure 10 Liquid–liquid phase transition temperature (T_{L-L}) and onset-crystallization temperature (T_{cry}) curves for solutions of i-PP and phthalates of dibutyl (C4), dihexyl (C6) and diheptyl (C7). T_{L-L} was obtained by optical microscopy with a hot stage and T_{cry} by DSC at a cooling rate of 10°C/min.

The phenomenon may be interpreted with the calculated phase diagrams of ternary solution, as shown before. The total polymer concentration of the polymer-rich phase at which melting point and binodal curves coincide decreases as the temperature increases in Figures 6–8. The increasing melting point with dilution is observed at a lower temperature for a given concentration of polymer with more favorable interaction in Figure 9, which can be explained by comparison between Figure 6 and Figure 7. The temperature at which L-L phase separation intersects the liquid–solid phase transition is lower at a given concentration of total polymer with a smaller χ.

CONCLUSIONS

Phase diagrams were calculated to investigate the effects of polydispersity of polymer molecules and interaction on the phase behavior of polydisperse i-PP solutions based on Flory-Huggins solution thermodynamics. The polydispersity was modeled with blends of two monodisperse polymers differing in chain lengths. It was found that the temperature at which L-L phase separation was coupled with liquid–solid phase equilibrium increased with decreasing concentration of total polymer due to polydispersity of polymer chain lengths, and this phenomenon was observed at a lower temperature with a more favorable interaction. The results were consistent with the experimental observations of i-PP solutions.

The simple model employed in this work explicitly explains the essential feature of the effect of polydispersity on the interference of the L-L phase separation and crystallization in i-PP solutions. The fractionation due to liquid demixing in the coupled phase transitions may significantly influence the complexity of multiphase structures in polymer–solvent mixtures for a polymer of broad molecular weight distribution. The pore size and its distribution of microporous polymeric membranes would be controlled more effectively by understanding these phenomena related to polydispersity.

H. K. Lee would like to thank Chungnam Sanup University for partial financial support of this study.

REFERENCES

1. R. E. Kesting, *Synthetic Polymeric Membranes, A Structural Perspective,* Wiley, New York, 1985, p. 261.
2. M. H. V. Mulder, *Basic Principles of Membrane Technology,* Kluwer Academic, Dordrecht, The Netherlands, 1991.
3. D. R. Lloyd, J. W. Barlow, and K. E. Kinzer, in *New Membrane Materials and Processes for Separation,* K. K. Sirkar and D. R. Lloyd, Eds., AICHE Symp. Ser., No. 261, AICHE, New York, 1988.
4. P. Witte, P. J. Dijkstra, J. W. A. Berg, and J. Feijen, *J. Membr. Sci.,* **117,** 1 (1996).
5. G. E. Gaides and A. J. McHugh, *Polymer,* **30,** 2118 (1989).
6. J. H. Aubert, *Macromolecules,* **21,** 3468 (1988).
7. H. C. Vadalia, H. K. Lee, A. S. Myerson, and K. Levon, *J. Membr. Sci.,* **89,** 37 (1994).
8. J. H. Aubert and R. L. Clough, *Polymer,* **26,** 2047 (1985).
9. H. K. Lee, A. S. Myerson, and K. Levon, *Macromolecules,* **25,** 4002 (1992).
10. L. Aerts, M. Kunz, H. Berghmans, and R. Koningsveld, *Makromol. Chem.,* **194,** 2697 (1993).
11. P. Vandeweerdt, H. Berghmans, and Y. Tervoort, *Macromolecules,* **24,** 3547 (1991).
12. P. J. Flory, *Principles of Polymer Chemistry,* Cornell University Press, Ithaca, NY, 1953.
13. H. Tompa, *Polymer Solutions,* Butterworths, London, 1956.

14. H. Tompa, *Trans. Faraday Soc.,* **45,** 1142 (1949).
15. R. Koningsveld and A. J. Staverman, *J. Polym. Sci., Polym. Phys. Ed.,* **6,** 305 (1968).
16. A. Abe and P. J. Flory, *Macromolecules,* **11,** 1122 (1978).
17. K. Kamide and Y. Miyazaki, *Polym. J.,* **12,** 205 (1980).
18. F. W. Altena and C. A. Smolders, *Macromolecules,* **15,** 1491 (1982).
19. L. Yilmaz and A. J. McHugh, *J. Appl. Polym. Sci.,* **31,** 997 (1986).
20. A. Nakajima and H. Fujiwara, *J. Polym. Sci., Polym. Phys. Ed.,* **6,** 723 (1968).
21. H. Tompa, *Trans. Faraday Soc.,* **46,** 970 (1950).
22. J. Brandrup and E. H. Immergut, Ed., *Polymer Handbook,* 3rd ed., John Wiley and Sons, New York, 1989.
23. A. Prasad and L. Mandelkern, *Macromolecules,* **22,** 914 (1989).
24. L. Wild, *Adv. Polym. Sci.,* **98,** 1 (1990).
25. W. R. Burghardt, *Macromolecules,* **22,** 2482 (1989).